0026-895X/06/6901-174–184$20.00
MOLECULAR PHARMACOLOGY
Copyright © 2006 The American Society for Pharmacology and Experimental Therapeutics
Mol Pharmacol 69:174–184, 2006

Vol. 69, No. 1
14258/3073294
Printed in U.S.A.

Altered Expression of $G_{q/11}\alpha$ Protein Shapes mGlu1 and mGlu5 Receptor-Mediated Single Cell Inositol 1,4,5-Trisphosphate and Ca^{2+} Signaling

Peter J. Atkinson, Kenneth W. Young, Steven J. Ennion, James N. C. Kew, Stefan R. Nahorski, and R. A. John Challiss

Department of Cell Physiology & Pharmacology, University of Leicester, Leicester, United Kingdom (P.J.A., K.W.Y., S.J.E., S.R.N., R.A.J.C.); and Psychiatry Centre of Excellence for Drug Discovery, GlaxoSmithKline, Harlow, United Kingdom (J.N.C.K.)

Received April 26, 2005; accepted October 18, 2005

ABSTRACT

The metabotropic glutamate (mGlu) receptors mGlu1 and mGlu5 mediate distinct inositol 1,4,5-trisphosphate (IP_3) and Ca^{2+} signaling patterns, governed in part by differential mechanisms of feedback regulation after activation. Single cell imaging has shown that mGlu1 receptors initiate sustained elevations in IP_3 and Ca^{2+}, which are sensitive to agonist concentration. In contrast, mGlu5 receptors are subject to cyclical PKC-dependent uncoupling and consequently mediate coincident IP_3 and Ca^{2+} oscillations that are largely independent of agonist concentration. In this study, we investigated the contribution of $G_{q/11}\alpha$ protein expression levels in shaping mGlu1/5 receptor-mediated IP_3 and Ca^{2+} signals, using RNA interference (RNAi). RNAi-mediated knockdown of $G_{q/11}\alpha$ almost abolished the single-cell increase in IP_3 caused by mGlu1 and mGlu5 receptor activation. For the mGlu1 receptor, this unmasked baseline Ca^{2+} oscillations that persisted even at maximal agonist concentrations. mGlu5 receptor-activated Ca^{2+} oscillations were still observed but were only initiated at high agonist concentrations. Recombinant overexpression of $G_q\alpha$ enhanced IP_3 signals after mGlu1 and mGlu5 receptor activation. It is noteworthy that although mGlu5 receptor-mediated IP_3 and Ca^{2+} oscillations in control cells were largely insensitive to agonist concentration, increasing $G_q\alpha$ expression converted these oscillatory signatures to sustained plateau responses in a high proportion of cells. In addition to modulating temporal Ca^{2+} signals, up- or down-regulation of $G_{q/11}\alpha$ expression alters the threshold for the concentration of glutamate at which a measurable Ca^{2+} signal could be detected. These experiments indicate that altering $G_{q/11}\alpha$ expression levels differentially affects spatiotemporal aspects of IP_3 and Ca^{2+} signaling mediated by the mGlu1 and mGlu5 receptors.

Activation of the phospholipase C (PLC) pathway via coupling of G protein-coupled receptors (GPCRs) to G proteins of the $G_{q/11}$ family results in inositol 1,4,5-trisphosphate (IP_3) production and mobilization of intracellular calcium ($Ca^{2+}{}_i$). Receptor activation can initiate spatially and temporally unique Ca^{2+} signals and thereby regulate an array of cellular processes (Berridge et al., 2000). In this study, we have investigated the contribution of $G_{q/11}\alpha$ protein expression in shaping receptor-initiated IP_3 and Ca^{2+} signaling patterns.

This work was supported by the Wellcome Trust of Great Britain (grant 062495) and by a joint Biotechnology and Biological Sciences Research Council and GlaxoSmithKline Ph.D. studentship (to P.J.A.).

Article, publication date, and citation information can be found at http://molpharm.aspetjournals.org.

doi:10.1124/mol.105.014258.

The group I metabotropic glutamate receptors mGlu1a and mGlu5a are family C GPCRs. mGlu1a and mGlu5a receptors couple preferentially to the major isoforms of the G_q family, $G_q\alpha$ and $G_{11}\alpha$, and are capable of activating distinct patterns of Ca^{2+} mobilization (Hermans and Challiss, 2001). Stimulation of the mGlu1a receptor predominantly initiates a peak-and-plateau Ca^{2+} response, whereas mGlu5a receptor activation mediates a Ca^{2+} oscillatory response over a broad range of stimulus strengths (Nash et al., 2002). Previous studies proposed that mGlu5 receptor-mediated Ca^{2+} oscillations occur because of feedback inhibition via PKC-dependent phosphorylation of a single threonine residue (Thr^{840}; Kawabata et al., 1996); however, very recent studies have shown that Thr^{840} is not phosphorylated but instead plays a

ABBREVIATIONS: PLC, phospholipase C; GPCR, G protein-coupled receptor; IP_3, inositol 1,4,5-trisphosphate; PKC, protein kinase C; eGFP, enhanced green fluorescent protein; eGFP-$PH_{PLC\delta}$, pleckstrin homology domain of PLCδ1 tagged with enhanced green fluorescent protein; CICR, Ca^{2+}-induced Ca^{2+}-release; mGlu, metabotropic glutamate; mACh, muscarinic acetylcholine; RNAi, RNA interference; CHO, Chinese hamster ovary; HEK, human embryonic kidney; siRNA, small interfering RNA; PAGE, polyacrylamide gel electrophoresis; PBS, phosphate-buffered saline; PCR, polymerase chain reaction; RT, reverse transcription; KHB, Krebs-Henseleit buffer; RFU, relative fluorescent units; AM, acetoxymethyl ester; RGS, regulator of G protein signaling.

structural/permissive role for the phosphorylation of an adjacent residue (Ser^{839}) by PKC (Kim et al., 2005). Similar PKC-dependent Ca^{2+} oscillations have also been described after glutamate activation of astrocytes (Codazzi et al., 2001) and activation of another family C GPCR, the Ca^{2+}-sensing receptor (Young et al., 2002). Use of the pleckstrin homology domain of phospholipase Cδ tagged with enhanced green fluorescent protein (eGFP-$PH_{PLC\delta}$) has enabled IP_3 oscillations underlying mGlu5a receptor-activated Ca^{2+} oscillations to be observed (Nash et al., 2001, 2002; Nahorski et al., 2003). These PKC-dependent Ca^{2+} oscillations (referred to as "dynamic uncoupling") are distinct from regenerative Ca^{2+}-induced Ca^{2+}-release (CICR), which is generated through an intrinsic property of the IP_3 receptor (Thomas et al., 1996; Taylor and Thorn, 2001). CICR oscillations can be maintained with a relatively low steady-state increase in IP_3, as observed after activation of the M_3 muscarinic acetylcholine (mACh) receptor with a low agonist concentration in the same cell background (Nash et al., 2001). Our previous studies exploring the determinants of mGlu5 receptor signaling led us to propose a model in which Ca^{2+} oscillation frequency is dependent on receptor expression levels but is largely independent of agonist concentration (Nash et al., 2002). However, the importance of receptor-G protein coupling efficiency in group I mGlu receptor-mediated Ca^{2+} signaling has not yet been investigated. It is clear that regulation and localization of $G_{q/11}\alpha$ proteins could be a key, influencing factor in shaping the Ca^{2+} signals produced.

Studies examining the role of $G_{q/11}\alpha$ proteins generally, and in conjunction with mGlu receptor signaling, have been facilitated greatly by the generation of $G_{q/11}\alpha$ knockout mice (for review, see Offermanns, 2003). However, gene deletion studies are limited by the mortality of $G_q\alpha/G_{11}\alpha$ double-knockout mice and also by the possibility that the phenotype of the cells studied may adapt to compensate for the loss of a particular Gα, as observed for the deletion of other G protein subtypes, including $G_o\alpha$ (Greif et al., 2000) and $G_{15}\alpha$ (Davignon et al., 2000). Other investigators have successfully used antisense methods to reduce $G_{q/11}\alpha$ expression; however, these studies often rely on microinjection, making an accurate determination of endogenous $G_q\alpha$ and $G_{11}\alpha$ protein expression difficult to ascertain (Macrez-Lepretre et al., 1997; Haley et al., 1998). Determining the relative $G_q\alpha$ and $G_{11}\alpha$ expression levels after knockdown is clearly desirable in this type of study. Distinct roles of $G_q\alpha$ and $G_{11}\alpha$ in mGlu1a receptor-mediated Ca^{2+} signaling in Purkinje neurons have recently been shown to result from differential expression levels of these two isoforms (Hartmann et al., 2004). Therefore, it was shown that $G_q\alpha$ was solely required for mGlu receptor-dependent synaptic transmission, whereas both $G_q\alpha$ and $G_{11}\alpha$ contributed to long-term depression in Purkinje neurons.

In the current study, we have used $G_{q/11}\alpha$-RNAi and $G_q\alpha$ overexpression in combination with single-cell IP_3 and Ca^{2+} imaging as a novel approach to investigate the role of $G_{q/11}\alpha$ expression in GPCR-mediated signaling. RNAi-knockdown of $G_{q/11}\alpha$ protein expression was initially characterized in HEK cells stably expressing recombinant M_3 mACh receptor. We then demonstrated the effects of RNAi and recombinant $G_q\alpha$ expression on IP_3 and Ca^{2+} signals generated by mGlu1 and mGlu5 receptors expressed recombinantly in CHO cells. By altering $G_{q/11}\alpha$ expression levels, the agonist concentration-dependencies of these G_qPCRs were changed. Furthermore, the temporal profiles of Ca^{2+} signals generated indicate a central role for $G_{q/11}\alpha$ in defining the nature of the response observed.

Materials and Methods

Cell Culture and Plasmid Transfection. CHO cells stably expressing the human mGlu1a or mGlu5a receptor under the control of the inducible LacSwitch-II system (Stratagene, La Jolla, CA) were maintained as described previously (Hermans et al., 1998; Nash et al., 2002) and are denoted as CHO-*lac*-mGlu1 or CHO-*lac*-mGlu5. HEK cells stably expressing the M_3 mACh receptor (HEK-m3) were created and maintained as described previously (Tovey and Willars, 2004). Plasmid containing the fusion construct between eGFP and the pleckstrin homology domain of PLCδ1 (eGFP-$PH_{PLC\delta}$) was kindly donated by T. Meyer (Stanford University, Stanford, CA).

For single cell imaging experiments, CHO-*lac*-mGlu1/5 or HEK-m3 cells were grown on 25-mm coverslips and cotransfected 72 h before experimentation with 1.8 μg of $G_{q/11}\alpha$-RNAi, control RNAi, or full-length human $G_q\alpha$ and 0.2 μg of eGFP-$PH_{PLC\delta}$ (for IP_3 imaging) or eGFP (for Ca^{2+} imaging) using 6 μl of GeneJuice (Novagen/EMD Biosciences, Madison, WI) per coverslip. For induction of maximal mGlu receptor expression in CHO cells, the medium was replaced with fresh culture medium containing 100 μM IPTG 18 to 20 h before experimentation. For standard SDS-PAGE immunoblotting, HEK-m3 cells were transfected in six-well plates 72 h before experimentation with 2 μg of $G_{q/11}\alpha$-RNAi or control RNAi using Lipofectamine 2000. CHO cells were transfected in flasks (175 cm^2) with 10 μg of $G_{q/11}\alpha$-RNAi or control RNAi using 30 μl of GeneJuice and after 24 h, cells were seeded into six-well plates for a further 48 h. For receptor biotinylation, real-time PCR and 6 M urea SDS-PAGE analysis, CHO cells were transfected using the Nucleofection system (Amaxa Biosystems, Gaithersburg, MD), according to the manufacturer's optimized protocol. In brief, 5×10^6 cells were transfected with 2 μg of control- or $G_{q/11}\alpha$-RNAi and Program U-23 on the Nucleofector, before seeding cells into six-well plates 72 h before experimentation.

RNAi Design and Preparation. To design an RNAi plasmid expressing $G_{q/11}\alpha$-specific small interfering RNA (siRNA), the mRNA sequences for human $G_q\alpha$ (GenBank accession number NM_002072) and $G_{11}\alpha$ (GenBank accession number NM_002067) were aligned to identify potential target sequences. Candidate 19-base pair sequences, homologous for both human $G_q\alpha$ and $G_{11}\alpha$ genes (and containing a G/C content of 40–60%) were identified, and gene specificity was checked using the BLASTN algorithm to search the GenBank sequence database. RNAi-expressing constructs for five selected sequences were created according to the manufacturer's instructions [using the *pSilencer* 1.0-U6 expression system; Ambion (Austin, TX)], and the knockdown of recombinantly expressed CFP-labeled $G_q\alpha$ was used to assess the effectiveness of these constructs (data not shown). The target sequence selected for $G_{q/11}\alpha$ silencing was 5′-GATGTTCGTGGACCTGAAC-3′, corresponding to positions 932 to 950 relative to the start codon of human G_q and G_{11} (denoted "$G_{q/11}$-RNAi"). Furthermore, an additional control RNAi construct was generated (using the nucleotide sequence 5′-GCTGACCCTGGAGAGTTCATC-3′), and is denoted "control RNAi".

Immunoblot Analysis. Levels of endogenous $G_{q/11}\alpha$ protein expression in HEK-m3 and CHO-*lac*-mGlu1a cells were determined by a standard Western blot protocol (Willets and Kelly, 2001) using a $G_{q/11}\alpha$-specific antibody at 1:5000 dilution (CQ, kindly donated by G. Milligan, University of Glasgow, Glasgow, UK). Antibodies against $G_{i1-3}\alpha$ (1:2000; Santa Cruz Biotechnology, Santa Cruz, CA), $G_{12}\alpha$ (1:1000; Santa Cruz Biotechnology) and γ-tubulin (1:10,000; Sigma, St. Louis, MO) were used as controls for RNAi specificity and protein loading. Antibodies against the C-terminal region of the mGlu1 receptor (1:1000; Chemicon International, Temecula, CA) and the

C-terminal region of the mGlu5 receptor (1:1000; Upstate Biotechnology, Lake Placid, NY), respectively, were used to detect mGlu1a and mGlu5a receptor expression. All primary antibody incubations were made at room temperature for 2 h or overnight at 4°C. Resolution of both $G_q\alpha$ and $G_{11}\alpha$ with an antibody (CQ) was achieved using SDS-PAGE gels containing 12.5% acrylamide and 6 M urea, as described previously (Milligan, 1993). The relative mobility of each Gα subunit was confirmed using cell lysates obtained from CHO-*lac*-mGlu cells recombinantly expressing human $G_q\alpha$ or $G_{11}\alpha$ using equivalent gels.

Cell-Surface Biotinylation of mGlu1a and mGlu5a Receptors. CHO-*lac*-mGlu1a and -mGlu5a cells were transiently transfected with $G_{q/11}\alpha$-RNAi, control RNAi, or full-length human $G_q\alpha$ using the Amaxa Nucleofection system, seeded into six-well plates, and induced 48 h later. After 72 h, cells were washed twice with PBS at room temperature and labeled with membrane-impermeant EZ-Link Sulfo-NHS-biotin (1 mM in PBS; Pierce, Rockford, IL) for 30 min at room temperature. Cells were washed twice with ice-cold PBS, once with 500 mM Tris/HCl, pH 7.4, and twice more with ice-cold PBS. Cells were then lysed for 10 min with solubilization buffer (10 mM Tris/HCl, 150 mM NaCl, 1 mM EDTA, 500 μM EGTA, 1% Igepal, and 0.1% SDS, pH 7.4) and centrifuged at 14,000*g* for 5 min. The cleared supernatant (900 μl) was then incubated with 200 μl of streptavidin/agarose beads (diluted 1:10 in solubilization buffer) for 2 h with constant rotation at 4°C. The remaining supernatant was retained to assess receptor expression in whole-cell lysates (see below). Beads were recovered by centrifugation during two washes with 1 ml of solubilization buffer and two washes with 1 ml of PBS. Immunocomplexes were dissociated with 50 μl of 2× sample buffer (125 mM Tris/HCl, 50 mM dithiothreitol, 4% SDS, 20% glycerol, 0.01% bromphenol blue, pH 6.8), heated at 90°C for 5 min, and then resolved by SDS-PAGE (as described above). For total cell extracts, 20 μl of the retained supernatant was diluted (1:1) with 2× sample buffer before SDS-PAGE.

PCR Amplification of the RNAi Target Region from CHO Cells. To determine the sequence of the RNAi target region of $G_q\alpha$ and $G_{11}\alpha$ derived from CHO cells, total RNA was isolated from CHO cells using the RNAeasy kit (QIAGEN, Valencia, CA). Samples (200 ng of RNA) were reverse-transcribed into cDNA using the Omniscript RT-PCR kit (QIAGEN). Primers specific for $G_q\alpha$ and $G_{11}\alpha$ based on rat sequence information (see Table 1) were used for PCR to amplify a 160-base pair fragment containing the RNAi target region using KOD HiFi DNA Polymerase (Novagen) as described in the manufacturer's instructions. PCR amplification was carried out over 30 cycles consisting of 98°C for 20 s, 50°C or 52°C (for $G_q\alpha$ and $G_{11}\alpha$ primers, respectively) for 20 s, and 72°C for 20 s. PCR reaction products were subsequently purified using a QIAquick PCR purification kit (QIAGEN); after gel electrophoresis, the PCR product was extracted and purified using a QIAEX II Gel extraction kit (QIAGEN). PCR products were sequenced directly using the same primers.

Quantitative Real-Time PCR. After RNAi transfection, total RNA and cDNA were prepared from samples in triplicate, as described above. An RT-negative control was included for each triplicate to control for genomic DNA contamination. Real-time PCR using SYBR-green fluorescence (Applied Biosystems, Foster City, CA) was carried out using an ABI PRISM 7700 sequence detection system as described previously (Medhurst et al., 2000). PCR parameters were 50°C for 2 min, 95°C for 10 min, 40 cycles of 95°C for 15 s, and 60°C for 1 min. Real-time PCR data were captured using Sequence Detector software (Applied Biosystems) to obtain threshold cycle values for the gene of interest. Values were normalized against a housekeeping gene, cyclophilin, and expressed as percentage of control. All measurements were performed in triplicate for three separate transfections using the Amaxa Nucleofection system.

Single Cell Imaging of IP_3. Increases in cellular IP_3 were detected by measuring the translocation of eGFP-$PH_{PLC\delta}$ from the plasma membrane to the cytosol as described previously (Nash et al., 2002; Young et al., 2003). Cells were transfected as described above, and coverslips were mounted on the stage of an Olympus IX70 inverted epifluorescence microscope and perfused (5 ml/min) at 37°C with Krebs-Henseleit buffer (KHB): 118 mM NaCl, 4.7 mM KCl, 1.2 mM $MgSO_4$, 1.3 mM $CaCl_2$, 1.2 mM KH_2PO_4, 4.2 mM $NaHCO_3$, 10 mM HEPES, and 11.7 mM glucose, pH 7.4) using a Gilson Minipuls 2 pump (Gilson, Inc., Middleton, WI). Confocal images were collected after excitation at 488 nm using an Olympus FV500 laser scanning confocal microscope at a scan rate of 1.5 to 2.5 Hz. eGFP-$PH_{PLC\delta}$ translocation was measured by creating a region of interest in the cytosol and plotting the average pixel intensity in that region versus time. Data are expressed in relative fluorescent units (RFU) by subtraction of background fluorescence followed by dividing the fluorescent intensity at a given time by the initial fluorescence within each region of interest (F/F_0). Drug applications were made using the perfusion line as indicated.

Ca^{2+} Imaging. Cells were transfected as described, and then loaded with fura-2 AM (Invitrogen) in 1 ml of KHB (final concentration, 5 μM) for 60 to 90 min. The cells were mounted on an inverted epifluorescence microscope (Diaphot; Nikon, Tokyo, Japan) with an oil immersion objective (40×) and then excited at 340 and 380 nm (for fura-2 AM) and 488 nm (for eGFP) using a Spectramaster II monochromator (PerkinElmer Life and Analytical Sciences, Boston, MA) at a sample rate of 0.7 Hz. GFP-containing cells were identified (as a marker of $G_{q/11}\alpha$-RNAi/control RNAi/$G_q\alpha$-transfected cells), and sequential images were then captured from GFP-transfected cells at wavelengths above 510 nm after drug applications made using the perfusion line as indicated. Ca^{2+} signals are expressed as 340 nm/380 nm ratios.

TABLE 1
Oligonucleotides
Oligonucleotide sequences are shown for sense (s) and antisense (as) primers.

Gene	GenBank Accession-Number	Primer	Sequence 5′-3′
Rat cyclophilin	NM_017101	s	TGTGCCAGGGTGGTGACTT
		as	CCACCAGTGCCATTATGGCGTGT
For real-time PCR			
$G_q\alpha$	NM_031036	s	AGTTCGAGTCCCCACCACAG
		as	CCTCCTACATCGACCATTCTGAA
$G_{11}\alpha$	NM_031033	s	GGTGGAGTCGGACAACGAGA
		as	GGGTAGGTGATGATTGTGCGG
For sequencing			
$G_q\alpha$	NM_031036	s	GGAGAAAATTATGTATTCC
		as	CTCCGTGTCTGTGGCACAC
$G_{11}\alpha$	NM_031033	s	AGACAAGATCCTGCACTCA
		as	TTCGGTGTCCGTGGCGCAG

Data Analysis. Curve fitting of data and calculation of EC_{50} values was carried out using Prism 3.0 (GraphPad Software, Inc., San Diego, CA). Statistical differences between data sets were determined by one-way analysis of variance for multiple comparisons, followed by Bonferroni's multiple-range test at $p < 0.05$ (using Prism 3.0 software), or Student's t test (unpaired; $p < 0.05$ being considered significant).

Results

RNAi-Mediated Knockdown of $G_{q/11}\alpha$ Protein Expression and Function in HEK Cells Stably Expressing the M_3 mACh Receptor. RNAi constructs designed using 19-base pair sequences targeting homologous regions of human $G_q\alpha$ and $G_{11}\alpha$ protein expression were initially tested in HEK-m3 cells. Immunoblotting experiments revealed robust silencing of $G_{q/11}\alpha$ 72 h after transfection with $G_{q/11}\alpha$-RNAi compared with control RNAi. In these experiments, the transfection efficiency typically achieved was ~50%, suggesting a high degree of $G_{q/11}\alpha$ silencing in individual HEK cells. Antibodies detecting γ-tubulin and G protein α-subunits, $G_{i1-3}\alpha$, confirmed equal protein loading (Fig. 1A).

Single-cell IP_3 imaging, using cells transfected with eGFP-$PH_{PLC\delta}$ alone, showed a concentration-dependent increase in cytosolic fluorescence in response to 30-s applications of methacholine, with a best-fit EC_{50} of 0.9 μM. This was unaffected by cotransfection with control RNAi but was inhibited by $G_{q/11}\alpha$-RNAi, as demonstrated by a rightward shift in the concentration-response curve (EC_{50} 6 μM) and a suppressed maximal response (2-fold, compared with 3.5-fold over basal in control cells, shown in Fig. 1B). Representative images (Fig. 1B) showed a clear suppression of eGFP-$PH_{PLC\delta}$ translocation from the plasma membrane to the cytosol in $G_{q/11}\alpha$-RNAi-containing cells compared with control RNAi and also indicate that these cells display no obvious morphological changes.

RNAi-Mediated Knockdown of $G_{q/11}\alpha$ Protein Expression in CHO Cells. Having identified a functional $G_{q/11}\alpha$-RNAi construct in HEK cells, we tested the same construct in CHO cell lines stably and inducibly expressing mGlu1 and mGlu5 receptors. Immunoblotting showed a significant inhibition of endogenous $G_{q/11}\alpha$ expression 72 h after transfection with $G_{q/11}\alpha$-RNAi compared with control RNAi cells (Fig. 2A). The transfection efficiency typically achieved in CHO cells was 40 to 50% (determined using green fluorescent protein; data not shown), again suggesting highly efficient $G_{q/11}\alpha$ protein silencing. It is noteworthy that $G_{i1-3}\alpha$, $G_{12}\alpha$, and γ-tubulin protein expression levels were unaffected (Fig. 2A). Further experiments confirmed that induction of mGlu1 and mGlu5 receptor expression was unaffected by RNAi treatment (Fig. 2B).

After the identification of an RNAi construct with $G_{q/11}\alpha$ silencing activity in both human and CHO cell backgrounds, the 19-base pair RNAi target sequence within $G_q\alpha$ and $G_{11}\alpha$ derived from the CHO cell line was investigated. No sequence information for Chinese hamster $G_{q/11}\alpha$ was available in the GenBank/EMBL databases. We therefore amplified the appropriate regions from CHO cells by PCR with $G_q\alpha$- and $G_{11}\alpha$-selective primers, based on rat sequence information (Table 1). Sequencing of the amplicons from CHO cells indicated two base pair differences (corresponding to C→T changes at positions 9 and 21 in Fig. 3A) in $G_{11}\alpha$ compared with CHO $G_q\alpha$ and human $G_{q/11}\alpha$.

In view of the contrasting reports of RNAi specificity in the literature, it was imperative to assess the knockdown of $G_q\alpha$ relative to $G_{11}\alpha$. Using the Nucleofection system to achieve optimal plasmid transfection (>80% determined using GFP;

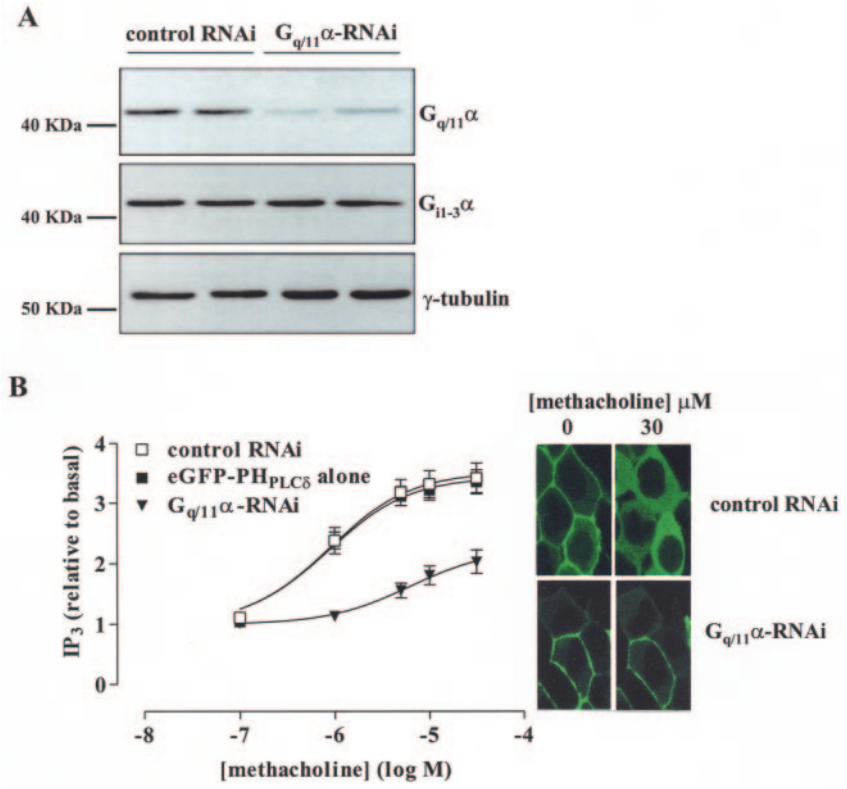

Fig. 1. RNAi-mediated knockdown of $G_{q/11}\alpha$ protein expression and function in HEK cells stably expressing the M_3 mACh receptor. The initial identification of an active $G_{q/11}\alpha$-RNAi construct was carried out in HEK cells transiently transfected (using Lipofectamine 2000) with control RNAi or $G_{q/11}\alpha$-RNAi 72 h before experimentation, as described under *Materials and Methods*. A, representative immunoblot demonstrating reduction of $G_{q/11}\alpha$ protein expression relative to control RNAi-transfected HEK cell lysates. Equal amounts of each sample were loaded in duplicate and also probed for $G_{i1-3}\alpha$ and γ-tubulin as a control for protein loading. B, effects of $G_{q/11}\alpha$-RNAi on M_3 mACh receptor function. Cells transfected (using GeneJuice) with eGFP-$PH_{PLC\delta}$ alone (39 cells) and in combination with $G_{q/11}\alpha$-RNAi (26 cells) or control RNAi (28 cells) were challenged for 30 s with increasing concentrations of methacholine. Cells were washed with KHB for 180 s between each addition. The peak changes in cytosolic eGFP-$PH_{PLC\delta}$ fluorescence were measured for each cell, and the data were averaged (mean ± S.E.M.) from at least three different experiments. Correlation coefficients of curve fits for eGFP-$PH_{PLC\delta}$ alone, and in combination with $G_{q/11}\alpha$-RNAi or control RNAi were 0.99, 0.99, and 1.0, respectively. Representative images show the effect of $G_{q/11}\alpha$ protein knockdown on single cell IP_3 production at a maximal concentration of methacholine.

data not shown) and real-time PCR with $G_q\alpha$- and $G_{11}\alpha$-specific primers (Table 1), a robust knockdown (~75%) of $G_q\alpha$ mRNA in both mGlu1 and mGlu5 receptor-expressing CHO-*lac* cells was observed (Fig. 3B). We were surprised to observe $G_{11}\alpha$ knockdown in the same experiments. $G_q\alpha$ and $G_{11}\alpha$ knockdown was normalized to cyclophilin mRNA levels, which were unaffected after $G_{q/11}\alpha$-RNAi transfection. To complement the mRNA analysis, SDS-PAGE gels containing 6 M urea were used to resolve $G_q\alpha$ and $G_{11}\alpha$ proteins in these cells (see *Materials and Methods*). Under these conditions, $G_{11}\alpha$ migrates farther than $G_q\alpha$, an observation confirmed using lysates obtained from CHO-*lac*-mGlu cells recombinantly expressing human $G_q\alpha$ and $G_{11}\alpha$ in equivalent gels (Fig. 3C). If the antibody immunoreactivity for both Gα subunits is comparable, these data suggest that expression levels of $G_q\alpha$ and $G_{11}\alpha$ proteins under control conditions in CHO-*lac*-mGlu1a cells are similar. The relative reduction of $G_q\alpha$ and $G_{11}\alpha$ protein expression was similar to the reduction in $G_q\alpha$ and $G_{11}\alpha$ mRNA levels determined by real-time PCR. A reduction of $G_q\alpha$ mRNA by ~75% corresponded to an almost complete knockout of $G_q\alpha$ protein; similarly, a reduction in $G_{11}\alpha$ mRNA by ~60% led to a slightly less efficient knockdown of $G_{11}\alpha$ protein expression. The relationship between mRNA and protein knockdown is dependent on the turnover of $G_q\alpha$ and $G_{11}\alpha$ proteins. A previous study in CHO cells reported that the half-time of $G_{q/11}\alpha$ is 18 h (Mitchell et al., 1993). Levels of $G_{i1-3}\alpha$, $G_{12}\alpha$, and γ-tubulin protein expression in these experiments were unaffected (data not shown). These experiments demonstrate the effectiveness of RNAi in silencing both $G_q\alpha$ and $G_{11}\alpha$ and so provide evidence that mismatches in the RNAi target sequence are tolerated, at least for these closely related gene products.

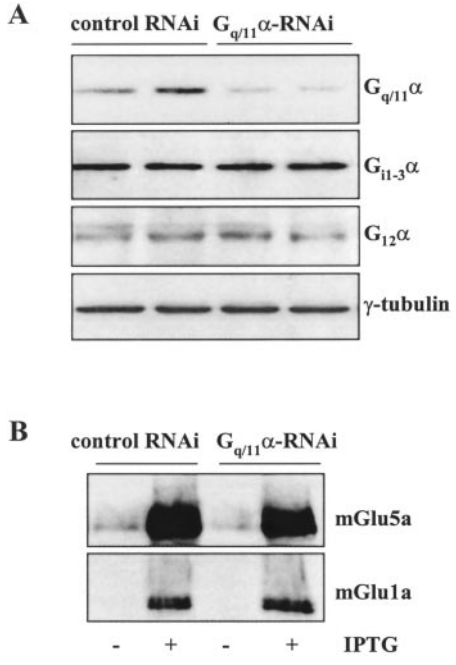

Fig. 2. RNAi-induced knockdown of $G_{q/11}\alpha$ protein expression in CHO cells. To assess the activity of the $G_{q/11}\alpha$-RNAi construct for use in CHO cell lines (where $G_q\alpha$ and $G_{11}\alpha$ sequence information was not available) stably expressing mGlu1 and mGlu5 receptors, cells were transfected (using GeneJuice) with control RNAi or $G_{q/11}\alpha$-RNAi 72 h before experimentation, as described under *Materials and Methods*. A, representative immunoblot showing reduction of $G_{q/11}\alpha$ protein expression relative to control RNAi-transfected CHO cell lysates. Equal amounts of each sample were loaded in duplicate as indicated after probing for $G_{i1-3}\alpha$, $G_{12}\alpha$, and γ-tubulin. B, representative immunoblot showing the induction of mGlu1 and mGlu5 receptor expression by 100 μM IPTG in control RNAi and $G_{q/11}\alpha$-RNAi transfected cells. Data are representative of at least three separate transfections.

Effects of Manipulating $G_{q/11}\alpha$ Expression on Cell-Surface Receptor Expression. To examine the possibility that up- or down-regulation of $G_{q/11}\alpha$ protein expression can influence mGlu1/5 receptor trafficking to the plasma membrane, we used a cell-surface protein biotinylation strategy. In both CHO-*lac*-mGlu1a (Fig. 4A) and mGlu5a (Fig. 4B) cells, $G_{q/11}\alpha$ protein expression was increased or decreased by transient transfection with human recombinant $G_q\alpha$ or $G_{q/11}\alpha$-RNAi, respectively. For mGlu1a and mGlu5a receptors, doublet immunoreactive bands were evident at ~150

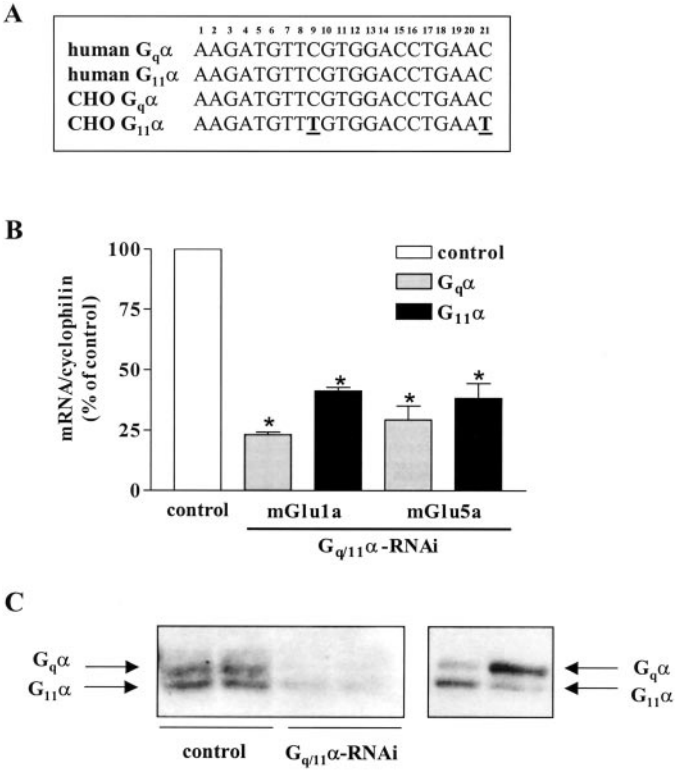

Fig. 3. Determining the specificity of $G_{q/11}\alpha$-RNAi-mediated knockdown of $G_q\alpha$ and $G_{11}\alpha$ mRNA and protein expression in CHO cells. A, sequencing $G_q\alpha$ and $G_{11}\alpha$ PCR products amplified from CHO cells. After the identification of an RNAi construct with $G_{q/11}\alpha$ silencing activity in both human and CHO cell backgrounds, the 19-base pair RNAi target sequence within $G_q\alpha$ and $G_{11}\alpha$ derived from the CHO cell line was confirmed. This region was amplified from CHO cells by PCR with $G_q\alpha$- and $G_{11}\alpha$-selective primers, based on rat sequence information (see Table 1). Shown is an alignment of the $G_q\alpha$ and $G_{11}\alpha$ PCR products from CHO cells with the equivalent human sequences to which the $G_{q/11}\alpha$-RNAi construct was targeted. B, quantitative real-time PCR analysis of $G_q\alpha$ and $G_{11}\alpha$ mRNA after $G_{q/11}\alpha$-RNAi transfection into CHO-*lac*-mGlu1 and -mGlu5 cells. Data are expressed as percentage of control after normalization to cyclophilin (mean ± S.E.M.; ∗, $p < 0.05$ compared with control). All measurements were performed in triplicate after three separate transfections using the Amaxa Nucleofection system. C, determining the relative knockdown of $G_q\alpha$ and $G_{11}\alpha$ protein expression levels after $G_{q/11}\alpha$-RNAi transfection. Lysates from the same transfected cells described in B were resolved by SDS-PAGE using a gel system containing 6 M urea to allow separation of $G_q\alpha$ from $G_{11}\alpha$ (see *Materials and Methods*). Immunodetection was carried out using antiserum CQ recognizing the conserved C-terminal region of both protein subunits. Shown are representative immunoblots, repeated at least three times, for ± $G_{q/11}\alpha$-RNAi effects (blot on left), and $G_q\alpha$ or $G_{11}\alpha$ overexpression in CHO-*lac*-mGlu cells (blot on right).

kDa. mGlu1a and mGlu5a receptor cell-surface biotinylation indicated that the mature, higher molecular weight protein (top band) is enriched at the plasma membrane (Fig. 4, A and B). It is noteworthy that altering $G_{q/11}\alpha$ expression levels did not affect cell-surface mGlu1a and mGlu5a receptor, or indeed total receptor expression in whole-cell extracts, indicating that the trafficking/localization of these receptors to the plasma membrane is independent of $G_{q/11}\alpha$ protein expression.

The Effects of Manipulating $G_{q/11}\alpha$ Protein Expression on Single Cell IP_3 Levels. Measurements of IP_3 production in cells transfected with $G_{q/11}\alpha$-RNAi, control RNAi, or full-length human $G_q\alpha$ were made possible by cotransfection of the IP_3 biosensor eGFP-$PH_{PLC\delta}$. In all of the control RNAi CHO-*lac*-mGlu1a cells examined, a graded increase in eGFP-$PH_{PLC\delta}$ translocation was observed in response to incremental glutamate concentrations, each applied for 30 s (Fig. 5), with a best-fit EC_{50} of 8.4 μM for the peak IP_3 response. In CHO-*lac*-mGlu1a cells transfected with $G_{q/11}\alpha$-RNAi, responses to glutamate were almost abolished, with no translocation of eGFP-$PH_{PLC\delta}$ observed in several individual cells. In contrast, when cells were transfected with full-length human $G_q\alpha$, the EC_{50} for the peak IP_3 response left-shifted from 8.4 to 2.0 μM glutamate ($p < 0.05$), whereas the maximal responsiveness was not significantly affected ($p > 0.05$; Fig. 5).

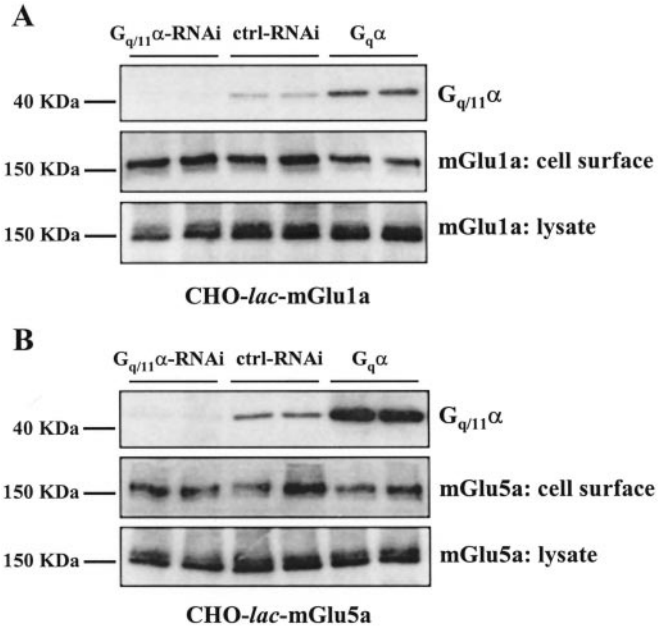

Fig. 4. Effect of $G_{q/11}\alpha$ protein manipulation on the cell-surface expression of mGlu1a and mGlu5a receptors. CHO-*lac*-mGlu1a (A) or CHO-*lac*-mGlu5a (B) cells were transiently transfected with $G_{q/11}\alpha$-RNAi, control-RNAi, or full-length human $G_q\alpha$ cDNA using the Amaxa Nucleofection system (see *Materials and Methods*) 72 h before experimentation. Shown are representative immunoblots from three experiments indicating $G_{q/11}\alpha$ protein and mGlu1a (A) or mGlu5a (B) receptor immunoreactivity using whole-cell lysates or after treatment of intact cell monolayers to biotinylate selectively cell-surface proteins.

Single-cell mGlu5a receptor-induced IP_3 responses underlying oscillatory Ca^{2+} signals have been studied extensively in CHO-*lac*-mGlu5a cells (Nash et al., 2002; Nahorski et al., 2003; Young et al., 2003). To examine the effect of manipulating $G_{q/11}\alpha$-protein levels, cells were transfected with $G_{q/11}\alpha$-RNAi, control RNAi, or full-length human $G_q\alpha$. Responses to a single maximal concentration (30 μM) of glutamate were subsequently examined over a 300-s time period for each treatment. Within a population of control cells, mGlu5a receptor-induced IP_3 increases in response to glutamate eGFP-$PH_{PLC\delta}$ translocation were not detected in 38% of cells (denoted "non-responders" in Fig. 6, A and B). In control RNAi cells in which eGFP-$PH_{PLC}\delta$ translocation was measurable, the predominant response was a peak elevation of IP_3 followed by repetitive oscillations until agonist washout (denoted as oscillatory in Fig. 6, A and B). In several cells (24% of the total number of cells), no detectable change in IP_3 was detected after the initial peak increase (denoted as a single spike in Fig. 6A). In CHO-*lac*-mGlu5a cells transfected with $G_{q/11}\alpha$-RNAi, repetitive oscillations in IP_3 were still observed. However, the number of nonresponders and single spike responses increased to 86% (from 62%) of the total number of cells. In contrast, after full-length $G_q\alpha$ transfection, the number of nonresponding cells decreased to 25% of the total population, and only a relatively low number of cells (8%) exhibited IP_3 oscillations. Instead, in 50% of $G_q\alpha$-transfected cells, IP_3 signals were manifested as an initial peak followed by a sustained plateau response until agonist washout (denoted as saturating in Fig. 6, A and B). In addition, the mean increase in peak IP_3 production was at least 2-fold higher in $G_q\alpha$-transfected cells (0.37 ± 0.07 RFU; $p < 0.05$), compared with control (0.17 ± 0.03 RFU) and RNAi-transfected cells (0.13 ± 0.05 RFU) (Fig. 6C).

$G_{q/11}\alpha$ Protein Expression Levels Influence Stimulus Strength and the Temporal Profile of mGlu Receptor-Mediated Ca^{2+} Mobilization. Previous studies from our laboratory have made real-time concurrent measurements of

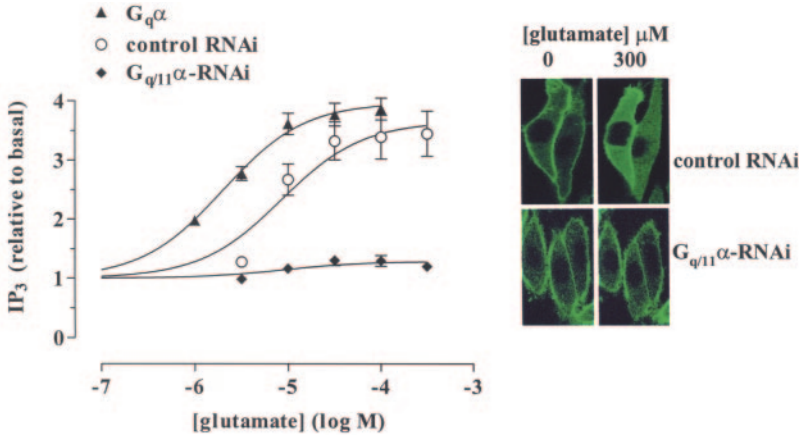

Fig. 5. The effect of $G_{q/11}\alpha$ protein manipulation on single-cell IP_3 responses in CHO-*lac*-mGlu1a cells. Cells cotransfected according to *Materials and Methods*, with eGFP-$PH_{PLC\delta}$ and $G_{q/11}\alpha$-RNAi (n = 18 cells), control RNAi (n = 23 cells) or full-length $G_q\alpha$ (n = 19 cells) were challenged for 30 s with increasing concentrations of glutamate. Cells were washed with KHB for 180 s between each addition. The peak changes in cytosolic eGFP-$PH_{PLC\delta}$ fluorescence were measured for each cell, and the data were averaged (mean ± S.E.M.) for separate cells from at least three different experiments. Representative images show the effect of RNAi-mediated knockdown of $G_{q/11}\alpha$ protein on mGlu1a receptor-mediated, single-cell IP_3 production, using a maximal concentration of glutamate. Correlation coefficients of curve fits for $G_{q/11}\alpha$-RNAi, control and full-length $G_q\alpha$-transfected cells were 0.77, 0.95, and 1.0, respectively.

mGlu1a receptor-generated IP_3 and $Ca^{2+}{}_i$ in single cells (Nash et al., 2001). During prolonged activation, these receptors give an initial transient peak in IP_3 production followed by a sustained plateau phase that is closely mirrored by a peak and sustained plateau Ca^{2+} response. In contrast, the mGlu5a receptor produces oscillatory IP_3 and Ca^{2+} signals (Nash et al., 2001, 2002; Nahorski et al., 2003). In the current study, the effects of manipulating $G_{q/11}\alpha$ protein levels on the glutamate concentration-dependence and temporal profile of mGlu1a and mGlu5a receptor-mediated Ca^{2+} signaling were investigated. Receptors were therefore exposed to incremental increases in glutamate (1 to 100 μM, 200 s at each concentration) to determine the role of $G_{q/11}\alpha$ expression levels on complex calcium signals.

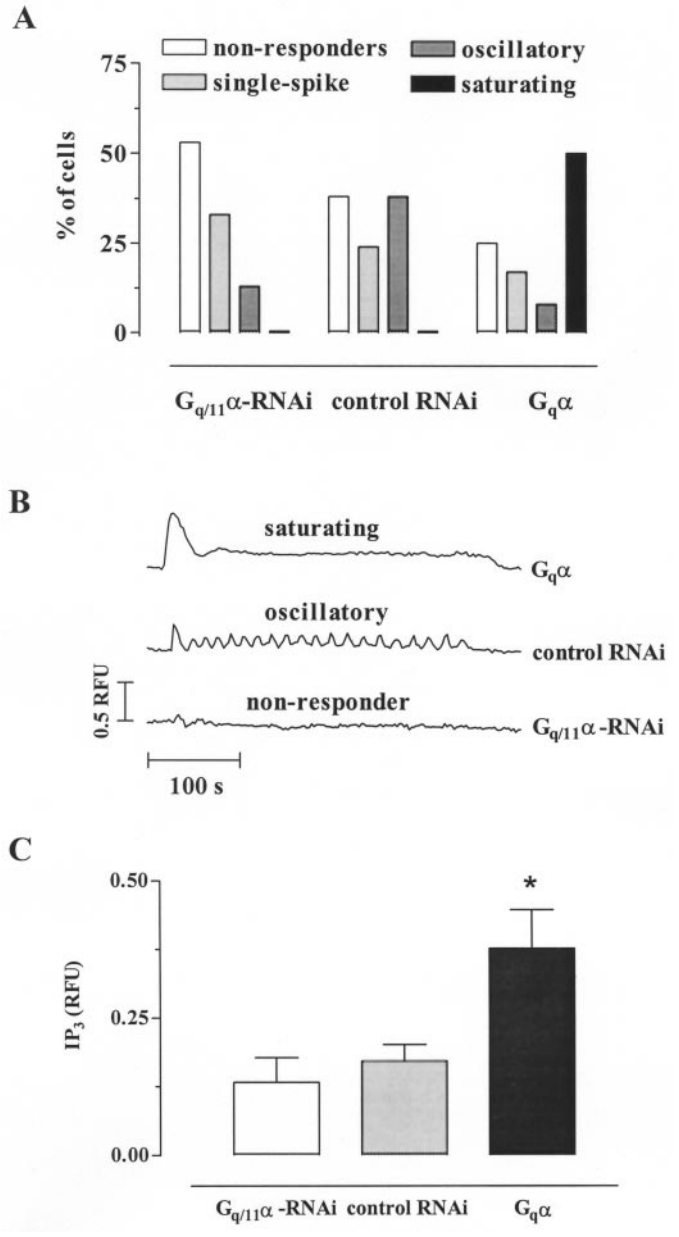

Fig. 6. The effect of $G_{q/11}\alpha$ protein manipulation on the temporal profile of single-cell IP_3 responses in CHO-*lac*-mGlu5a cells. Cells were cotransfected with eGFP-$PH_{PLC\delta}$ and $G_{q/11}\alpha$-RNAi (n = 15 cells), control RNAi (n = 34 cells), or full-length $G_q\alpha$ (n = 24 cells) 72 h before experimentation (see *Materials and Methods*). Because of the relatively small size of mGlu5a-receptor-mediated IP_3 responses at a single-cell level, a single maximal concentration of glutamate (30 μM) was perfused for 3 min allowing temporal changes in IP_3 production to be measured. Shown is a summary of responses taken from a total of 73 cells on three separate days (A). In several cells, responses were nominal, so that changes in fluorescence were not detected, and these are indicated as nonresponders. Cells that exhibited a single initial increase in IP_3 are indicated as single-spike responses. Other responses were classified in accordance with the representative traces shown, where oscillatory and saturating IP_3 signals were recorded from control RNAi and $G_q\alpha$-expressing cells, respectively (B). C, effect of changing $G_{q/11}\alpha$ protein expression on peak IP_3 (mean ± S.E.M. for all cells, including nonresponders; *, $p < 0.05$ compared with control).

In control RNAi and $G_q\alpha$-expressing CHO-*lac*-mGlu1a cells, ~60% of transfected cells responded to glutamate with an initial peak elevation in Ca^{2+} followed by a sustained plateau phase. After $G_{q/11}\alpha$-RNAi transfection, however, 84% (66 of 79) of cells elicited transient peak increases in Ca^{2+} mobilization without a sustained phase even at maximal concentrations of glutamate (Fig. 7C, denoted as "non-saturating"). These nonsaturating responses most often occurred as a single baseline spike coincident with agonist addition (as illustrated with the representative trace in Fig. 7A). On occasion, however, additional intermittent spikes were evident, perhaps signifying oscillations occurring as a result of regenerative CICR. The few cells that actually initiated a sustained peak and plateau did so only at high concentrations of agonist (7 of 66 cells over four experiments). Changing levels of $G_{q/11}\alpha$-protein expression altered the glutamate concentration threshold for the onset of mGlu1a receptor-induced Ca^{2+} responses (Fig. 8A). Thus, in control RNAi cells, the initial onset of Ca^{2+} mobilization occurred at either 3 or 10 μM glutamate (35 and 50% of the total number of cells, respectively), which correlates with the IP_3 measurements made in these cells (Fig. 5). In $G_{q/11}\alpha$-RNAi transfected cells, a greater agonist concentration was required to produce significant increases in IP_3 (around 10 μM glutamate), reflecting a shift to higher agonist concentrations for the onset of Ca^{2+} mobilization (only 14% responded to 3 μM but 53% responded to 10 μM). Furthermore, 25% of $G_{q/11}\alpha$-RNAi-transfected cells compared with 8% of control cells responded only to concentrations greater than 10 μM glutamate. The shift in stimulus threshold was further exemplified in experiments using $G_q\alpha$ overexpression, where 3 μM glutamate mediated a large increase in IP_3 (Fig. 5), so that 74% (25 of 34) of cells at this concentration of glutamate were able to initiate a Ca^{2+} signal compared with 35% of control cells (Figs. 7 and 8A). In the mGlu1a model system, $G_{q/11}\alpha$ expression levels clearly regulate the efficacy and the nature of agonist-mediated receptor activation. This is manifested as altered levels of IP_3 production and hence differential Ca^{2+} signals in response to increasing agonist concentrations. In contrast, mGlu5a receptor signaling is relatively independent of stimulus-strength over a wide agonist concentration range (Nash et al., 2002), and it was not clear what effect alterations in $G_{q/11}\alpha$ protein levels would have.

In control RNAi mGlu5a receptor-expressing cells, increasing concentrations of glutamate produced nonsaturating Ca^{2+} oscillations (Fig. 7, B and D). Although in many cells the frequency of Ca^{2+} oscillations was initially sensitive to the increase in agonist concentration, in all cases, the Ca^{2+} frequency quickly became insensitive to agonist concentration, which is indicative of oscillations driven by PKC-dependent feedback on the receptor (see Nash et al., 2002; Fig. 7B, representative trace). Similar observations were made from

mGlu5a receptor-expressing cells transfected with $G_{q/11}\alpha$-RNAi, but in the majority of cells, the onset of response occurred at higher concentrations of agonist (Fig. 8B; 10 μM versus 3 μM glutamate in control cells); consequently, non-saturating Ca^{2+} oscillations in most $G_{q/11}\alpha$-RNAi-transfected cells could not be identified until concentrations of $\geq$10 μM were used (Fig. 7, representative trace). In CHO-*lac*-mGlu5a cells transfected with $G_q\alpha$ 75% (52 of 69 cells) cells responded at 1 μM glutamate. A key effect of $G_q\alpha$ overexpression was the observation of mGlu5 cells exhibiting saturating Ca^{2+} responses to increasing concentrations of glutamate (Fig. 7, B and D). Thus, although oscillatory responses were observed at low glutamate concentrations, these rapidly converted to a sustained plateau response upon increases in agonist concentrations. In this way, the Ca^{2+} response mirrored the IP_3 signals produced by the mGlu5a receptor in recombinant $G_q\alpha$-expressing cells (Fig. 6B).

Discussion

Complex $G_{q/11}$-coupled receptor-mediated Ca^{2+} signals enable a wide range of cellular processes to be regulated (Berridge et al., 2000). Low levels of receptor occupancy are known to induce small steady-state increases in IP_3 that evoke oscillatory Ca^{2+} signals, the frequency of which is sensitive to agonist concentration. Higher levels of IP_3 generation caused by more intense receptor stimulation can lead to larger, peak-and-plateau–type Ca^{2+} responses. Studies using the IP_3 biosensor eGFP-$PH_{PLC\delta}$ have since shown that Ca^{2+} oscillations can also occur in synchrony with IP_3 oscil-

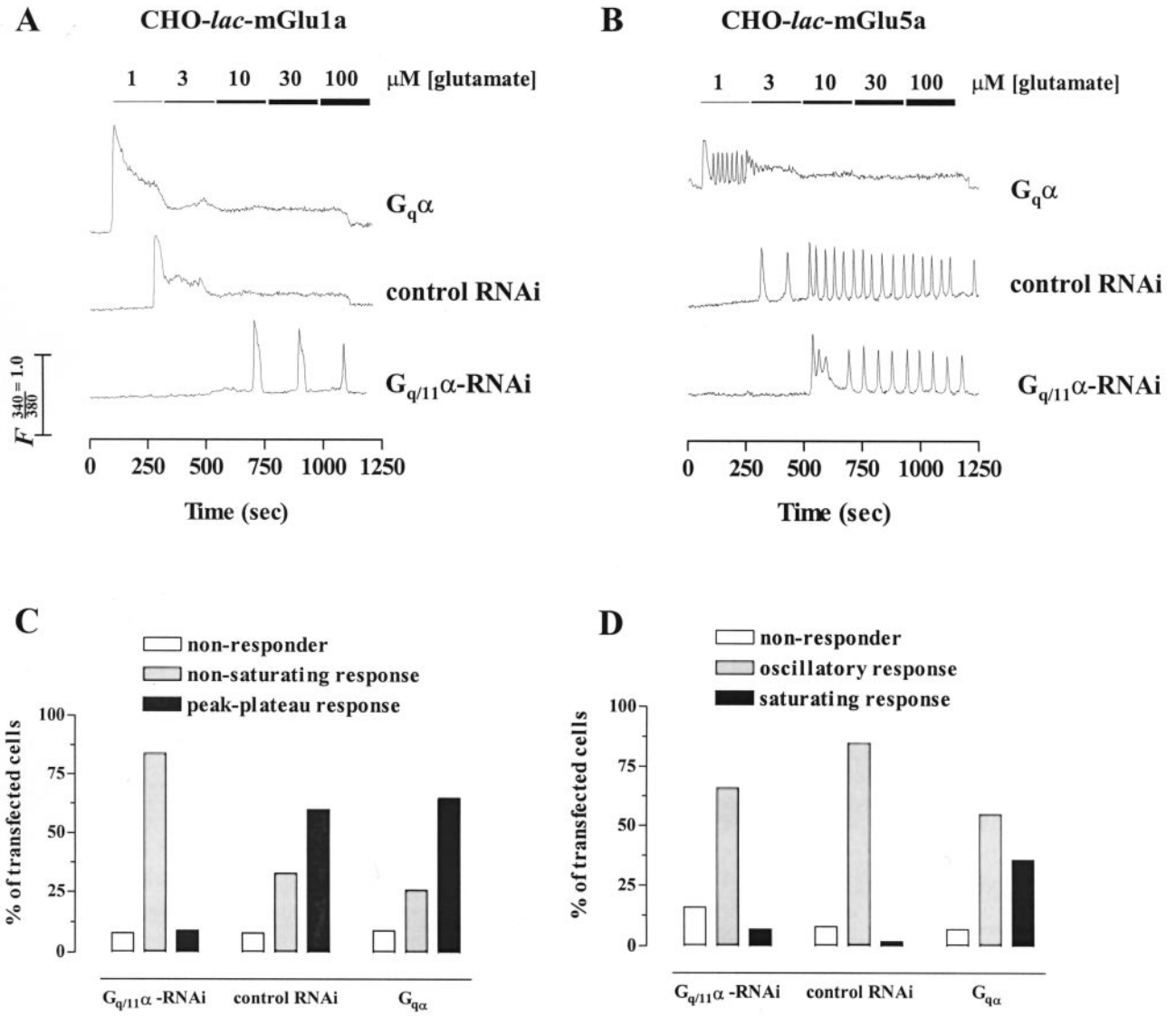

Fig. 7. Changes in $G_{q/11}\alpha$ protein expression level alter the temporal profile of Ca^{2+} signaling after group I mGlu receptor activation. CHO-*lac*-mGlu1a or mGlu5a cells cotransfected with eGFP and $G_{q/11}\alpha$-RNAi, control RNAi, or full-length $G_q\alpha$ were loaded with fura-2 AM, and single-cell images of changes in intracellular free Ca^{2+} concentration ($[Ca^{2+}]_i$) were measured from GFP-containing cells using an inverted epifluorescence microscope (*Materials and Methods*). Each concentration of the agonist glutamate was applied for 200 s. Shown are representative traces taken from single mGlu1a (A) or mGlu5a (B) receptor-expressing CHO cells after each treatment. After $G_{q/11}\alpha$-RNAi transfection, mGlu1a-expressing cells were largely unable to maintain the peak and plateau responses typically displayed in control RNAi cells and are therefore denoted as "nonsaturating" (C). In CHO-*lac*-mGlu5a cells overexpressing $G_q\alpha$, Ca^{2+} elevations were often sustained instead of displaying the characteristic PKC-dependent oscillatory responses; these are indicated as "saturating" responses (D). The Ca^{2+} signatures (classified according to the response achieved at 100 μM glutamate) obtained from 34 to 82 cells for each condition in both cell lines over four separate experiments are summarized in histograms as shown (C and D).

lations, as described in ATP-stimulated canine kidney epithelial cells (Hirose et al., 1999) or stimulation of mGlu5 receptors in CHO cells (Nash et al., 2001). Oscillations in IP_3 are likely to occur as a result of negative feedback regulation by PKC (Codazzi et al., 2001; Nash et al., 2002; Young et al., 2002) or RGS proteins (Luo et al., 2001) but also by a positive feedback effect of Ca^{2+} to enhance PLC activity (Young et al., 2003). For the mGlu5a receptor, synchronous IP_3 and Ca^{2+} oscillations occur via a PKC-dependent dynamic uncoupling of the receptor from its G protein by phosphorylation of a specific residue on the receptor (Kawabata et al., 1996; Kim et al., 2005). Because the substrate for PKC is the receptor, this provides a mechanism by which the frequency of Ca^{2+} oscillations are regulated by receptor density in addition to agonist concentration, as shown for the mGlu5 receptor (Nash et al., 2002). The mGlu1 receptor lacks this critical consensus sequence and is not subject to this feedback regulation. Therefore, mGlu1 receptor activation can initiate sustained peak-and-plateau Ca^{2+} responses. These studies suggest that Ca^{2+} signals initiated by $G_{q/11}$-coupled GPCRs are susceptible to regulation by a number of factors, including receptor-G protein coupling efficiency, receptor density, agonist concentration and sensitivity to feedback mechanisms.

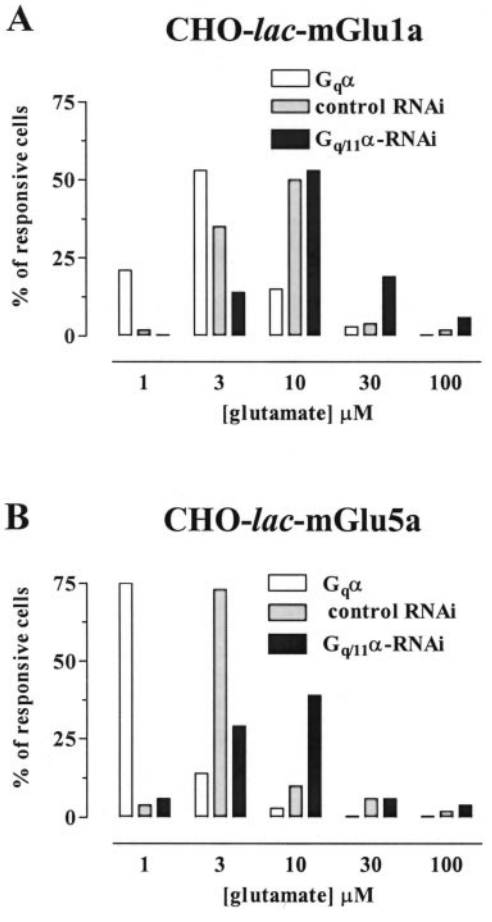

Fig. 8. Manipulating $G_{q/11}\alpha$ expression alters the agonist-concentration threshold for mGlu1a and mGlu5a receptor-mediated signaling. mGlu receptor-mediated Ca^{2+} responses from the same experiments described in Fig. 7 were further analyzed to determine onset of Ca^{2+} signaling events. Histograms indicate the number of mGlu1 (A) or mGlu5 (B) receptor-expressing cells (as a percentage of the total) that are responding for the first time.

The fine-tuning of Ca^{2+} signals by these factors may account for contrasting patterns of mGlu5 receptor-driven Ca^{2+} oscillations in different cell backgrounds (Codazzi et al., 2001; Dale et al., 2001; Nash et al., 2002). In the current study, we have extended these investigations by assessing the contribution of $G_{q/11}\alpha$ protein expression levels in generating distinct IP_3 and Ca^{2+} signaling patterns mediated by group I mGlu receptors. Using RNAi or recombinant $G_q\alpha$ expression in combination with an IP_3 biosensor or Ca^{2+} sensitive dye, we have been able to study the concentration-dependence and the temporal profile of IP_3 and $Ca^{2+}{}_i$ in single cells in real-time.

The use of RNAi as an approach to gene silencing is now extensive, although its mechanism is not yet fully understood (Dykxhoorn et al., 2003; Hannon and Rossi, 2004; Meister and Tuschl, 2004). The enormous interest in this technique has also highlighted potential limitations, in particular with respect to RNAi specificity (Hannon and Rossi, 2004; Snove and Holen, 2004). Here, we have shown a robust RNAi-induced silencing of $G_{q/11}\alpha$ protein expression in HEK-m3 cells that resulted in a suppression of the methacholine-induced IP_3 signal. Very recently, effective silencing of $G_{q/11}\alpha$ proteins in HEK cells has been reported in two other studies, using an RNAi sequence identical to the one used here. Using an siRNA approach, the authors established a role for $G_{q/11}\alpha$ proteins in stress fiber formation (Barnes et al., 2005), but not chemotaxis (Hunton et al., 2005), after angiotensin II AT_{1A} receptor activation.

Effective $G_{q/11}\alpha$ silencing was also observed in CHO-*lac* cell lines stably expressing mGlu1 or mGlu5 receptors, with no effect on the expression levels of $G_{i1-3}\alpha$ and $G_{12}\alpha$ proteins or the receptors themselves. Despite the presence of a 2-base-pair mismatch in the RNAi target region of $G_{11}\alpha$ compared with $G_q\alpha$ in the Chinese hamster cell model, real-time PCR and a pan-$G_{q/11}\alpha$ antibody revealed knockdown of both $G_q\alpha$ and $G_{11}\alpha$. Several reports have described similar tolerance of mismatches between siRNA and target mRNA, especially when these occur at the periphery of the target sequence (Amarzguioui et al., 2003; Vickers et al., 2003; Snove and Holen, 2004). Other studies also indicate that siRNAs containing mismatches can act as endogenous micro-RNAs to inhibit translation, but not to cause significant mRNA degradation (Doench et al., 2003; Saxena et al., 2003). However, this was not the case here, in that we observed a clear reduction in mRNA and protein expression. The effect therefore seems to be specific to $G_q\alpha$ and $G_{11}\alpha$ as a result of the close homology of the two sequences in the target region, instead of generic knockdown of unrelated proteins. In this study, we have therefore been able to use the RNAi construct to assess the effects of combined $G_{q/11}\alpha$ knockdown, but in doing so also provide evidence for a "cross-reactivity" of siRNA targeting closely related genes.

Knockdown of $G_{q/11}\alpha$ protein almost completely eliminated mGlu1a receptor-mediated IP_3 responses in single cells at maximal concentrations of agonist, whereas increased $G_q\alpha$ expression produced a significant enhancement in agonist sensitivity. Despite the ability of mGlu1a receptors to couple to other G proteins, such as $G_i\alpha$, which can contribute to phosphoinositide turnover (Hermans and Challiss, 2001), our current data suggest that $G_{q/11}\alpha$ coupling alone accounts for the majority of PLC activation in this expression system. Reducing the expression level of $G_{q/11}\alpha$ clearly affected the

signaling properties of mGlu1a receptor, so that the subsequent Ca^{2+} response no longer resembled the characteristic sustained peak-and-plateau signal typical of this receptor subtype (Kawabata et al., 1996; Nash et al., 2001). Instead, the observed baseline Ca^{2+} spiking was likely to be the result of regenerative CICR associated with small increments in IP_3 (Bootman et al., 1996; Thomas et al., 1996; Nash et al., 2001; Young et al., 2003). This finding supports the notion that the temporal response initiated by the mGlu1a receptor is dependent on stimulus strength and is likely to be influenced by receptor *and* G protein expression levels.

Ca^{2+} signals activated by the mGlu5 receptor were also sensitive to changes in $G_{q/11}\alpha$ expression. Using recombinant $G_q\alpha$ expression, we have revealed an ability of mGlu5 receptor to overcome PKC-dependent feedback allowing the receptor to mediate plateau IP_3 and Ca^{2+} responses. In cells transfected with recombinant $G_q\alpha$, peak IP_3 responses were clearly enhanced, and Ca^{2+} mobilization was achieved at lower threshold concentrations of agonist. This supports our previous proposal (Nash et al., 2002) and suggests that increased PLC activation reduces the period of PKC-dependent uncoupling and favors transition to sustained Ca^{2+} mobilization. With increased coupling and PLC activation, the mGlu5 receptor therefore mirrors M_3 mACh receptor signaling in lacrimal acinar cells, where PKC feedback occurs over a defined agonist concentration range (Bird et al., 1993). It is likely that sustained activation occurs when IP_3 receptors are saturated, leading to store depletion and capacitative Ca^{2+} entry. Indeed, previous studies have demonstrated mGlu5 receptor-activated peak-and-plateau responses in the CHO-*lac*-mGlu5a cell-model after thapsigargin-induced depletion of intracellular Ca^{2+} stores (Nash et al., 2002). Using RNAi, we have shown that a reduction in mGlu5 receptor stimulus-strength restricts IP_3 production, even at maximal concentrations of agonist, and constrains Ca^{2+} responses to baseline oscillations that require higher concentrations of agonist for initiation. Although PKC dependence was not tested here, previous studies in the same cells have shown that PKC down-regulation can prevent IP_3 oscillations, such that maximal concentrations of agonist initiate sustained peak-and-plateau Ca^{2+} responses in a similar manner to the mGlu1a receptor (Nash et al., 2002). It is noteworthy that at lower concentrations of agonist, PKC-independent Ca^{2+} oscillations were seen that were sensitive to agonist concentration and may reflect the Ca^{2+} oscillations observed in some cells after RNAi treatment in the present experiments.

In conclusion, we have shown that altering $G_{q/11}\alpha$ expression markedly alters the temporal profile and agonist concentration-dependencies of IP_3 and Ca^{2+} signals generated after either mGlu1a or mGlu5a receptor activation. This work also demonstrates that regulating $G_{q/11}\alpha$ expression levels can fundamentally alter the signaling properties of the mGlu5 receptor subtype. For the mGlu5 receptor, it seems that the predominant dynamic uncoupling mechanism linking receptor activation to Ca^{2+} signaling instills particular emergent properties. Thus, whereas the receptor expression level primarily determines the Ca^{2+} oscillatory frequency, the transitions between CICR, dynamic uncoupling, and peak-and-plateau behaviors are modulated by the level of $G_{q/11}$ expression. It will be interesting to establish the effects of changing the levels of other intermediates in the signaling pathway (e.g., PLCβ expression) or the presence of Homer proteins (Fagni et al., 2000; Kiselyov et al., 2003) on mGlu1/5 receptor signaling. It is also interesting to speculate on whether translocation of mGlu5 receptors to the plasma membrane from an intracellular locus (Hubert et al., 2001) and/or direct or indirect (e.g., through changes in RGS protein expression) changes in G protein expression/function can fundamentally alter neuronal Ca^{2+} signaling by this receptor subtype under altered physiological or pathophysiological conditions.

Acknowledgments

We thank Drs. Melanie Robbins, Isabel Benzel, and Andrew Calver (GlaxoSmithKline, Harlow, UK) for expert technical guidance on RT-PCR and helpful discussion. We also thank Dr. Mark Nash (Novartis Institute of Medical Sciences, London, UK) for initial input and ongoing intellectual contribution to this research project.

References

Amarzguioui M, Holen T, Babaie E, and Prydz H (2003) Tolerance for mutations and chemical modifications in a siRNA. *Nucleic Acids Res* **31:**589–595.
Barnes WG, Reiter E, Violin JD, Ren X-R, Milligan G, and Lefkowitz RJ (2005) β-Arrestin 1 and $G\alpha_{q/11}$ coordinately activate RhoA and stress fiber formation following receptor stimulation. *J Biol Chem* **280:**8041–8050.
Berridge MJ, Lipp P, and Bootman MD (2000) The versatility and universality of calcium signalling. *Nat Rev Mol Cell Biol* **1:**11–21.
Bird GS, Rossier MF, Obie JF, and Putney JW (1993) Sinusoidal oscillations in intracellular calcium requiring negative feedback by protein kinase C. *J Biol Chem* **268:**8425–8428.
Bootman MD, Young KW, Young JM, Moreton RB, and Berridge MJ (1996) Extracellular calcium concentration controls the frequency of intracellular calcium spiking independently of inositol 1,4,5-trisphosphate production in HeLa cells. *Biochem J* **314:**347–354.
Codazzi F, Teruel MN, and Meyer T (2001) Control of astrocyte Ca^{2+} oscillations and waves by oscillating translocation and activation of protein kinase C. *Curr Biol* **11:**1089–1097.
Dale LB, Babwah AV, Bhattacharya M, Kelvin DJ, and Ferguson SSG (2001) Spatial-temporal patterning of metabotropic glutamate receptor-mediated inositol 1,4,5-triphosphate, calcium and protein kinase C oscillations: protein kinase C-dependent receptor phosphorylation is not required. *J Biol Chem* **276:**35900–35908.
Davignon I, Catalina MD, Smith D, Montgomery J, Swantek J, Croy J, Siegelman M, and Wilkie TM (2000) Normal hematopoiesis and inflammatory responses despite discrete signaling defects in $G\alpha_{15}$ knockout mice. *Mol Cell Biol* **20:**797–804.
Doench JG, Petersen CP, and Sharp PA (2003) siRNAs can function as miRNAs. *Genes Dev* **17:**438–442.
Dykxhoorn DM, Novina CD, and Sharp PA (2003) Killing the messenger: short RNAs that silence gene expression. *Nat Rev Mol Cell Biol* **4:**457–467.
Fagni L, Chavis P, Ango F, and Bockaert J (2000) Complex interactions between mGluRs, intracellular Ca^{2+} stores and ion channels in neurons. *Trends Neurosci* **23:**80–88.
Greif GJ, Sodickson DL, Bean BP, Neer EJ, and Mende U (2000) Altered regulation of potassium and calcium channels by $GABA_B$ and adenosine receptors in hippocampal neurons from mice lacking $G\alpha_o$. *J Neurophysiol* **83:**1010–1018.
Haley JE, Abogadie FC, Delmas P, Dayrell M, Vallis Y, Milligan G, Caulfield MP, Brown DA, and Buckley NJ (1998) The α-subunit of G_q contributes to muscarinic inhibition of the M-type potassium current in sympathetic neurons. *J Neurosci* **18:**4521–4531.
Hannon GJ and Rossi JJ (2004) Unlocking the potential of the human genome with RNA interference. *Nature (Lond)* **431:**371–378.
Hartmann J, Blum R, Kovalchuk Y, Adelsberger H, Kuner R, Durand GM, Miyata M, Kano M, Offermanns S, and Konnerth A (2004) Distinct roles of $G\alpha_q$ and $G\alpha_{11}$ for Purkinje cell signaling and motor behavior. *J Neurosci* **24:**5119–5130.
Hermans E and Challiss RA (2001) Structural, signalling and regulatory properties of the group I metabotropic glutamate receptors: prototypic family C G-protein-coupled receptors. *Biochem J* **359:**465–484.
Hermans E, Young KW, Challiss RAJ, and Nahorski SR (1998) Effects of human type 1a metabotropic glutamate receptor expression level on phosphoinositide and Ca^{2+} signalling in an inducible cell expression system. *J Neurochem* **70:**1772–1775.
Hirose K, Kadowaki S, Tanabe M, Takeshima H, and Iino M (1999) Spatiotemporal dynamics of inositol 1,4,5-trisphosphate that underlies complex Ca^{2+} mobilization patterns. *Science (Wash DC)* **284:**1527–1530.
Hubert GW, Paquet M, and Smith Y (2001) Differential subcellular localization of mGluR1a and mGluR5a in the rat and monkey Substantia nigra. *J Neurosci* **21:**1838–1847.
Hunton DL, Barnes WG, Kim J, Ren X-R, Violin JD, Reiter E, Milligan G, Patel DD, and Lefkowitz RJ (2005) β-Arrestin 2-dependent angiotensin II type 1A receptor-mediated pathway of chemotaxis. *Mol Pharmacol* **67:**1229–1236.
Kawabata S, Tsutsumi R, Kohara A, Yamaguchi T, Nakanishi S, and Okada M (1996) Control of calcium oscillations by phosphorylation of metabotropic glutamate receptors. *Nature (Lond)* **383:**89–92.
Kim CH, Braud S, Isaac JT, and Roche KW (2005) Protein kinase C phosphorylation of the metabotropic glutamate receptor mGluR5 on serine-839 regulates Ca^{2+} oscillations. *J Biol Chem* **280:**25409–25415.

Kiselyov K, Shin DM, and Muallem S (2003) Signalling specificity in GPCR-dependent Ca^{2+} signalling. *Cell Signal* **15:**243–253.
Luo X, Popov S, Bera AK, Wilkie TM, and Muallem S (2001) RGS proteins provide biochemical control of agonist-evoked $[Ca^{2+}]_i$ oscillations. *Mol Cell* **7:**651–660.
Macrez-Lepretre N, Kalkbrenner F, Schultz G, and Mironneau J (1997) Distinct functions of G_q and G_{11} proteins in coupling α_1-adrenoreceptors to Ca^{2+} release and Ca^{2+} entry in rat portal vein myocytes. *J Biol Chem* **272:**5261–5268.
Medhurst AD, Harrison DC, Read SJ, Campbell CA, Robbins MJ, and Pangalos MN (2000) The use of TaqMan RT-PCR assays for semi-quantitative analysis of gene expression in CNS tissues and disease models. *J Neurosci Methods* **98:**9–20.
Meister G and Tuschl T (2004) Mechanisms of gene silencing by double-stranded RNA. *Nature (Lond)* **431:**343–349.
Milligan G (1993) Regional distribution and quantitative measurement of the phosphoinositidase C-linked guanine nucleotide binding proteins $G_{11}\alpha$ and $G_q\alpha$ in rat brain. *J Neurochem* **61:**845–851.
Mitchell FM, Buckley NJ, and Milligan G (1993) Enhanced degradation of the phosphoinositidase C-linked guanine-nucleotide-binding protein $G_q\alpha/G_{11}\alpha$ following activation of the human M_1 muscarinic acetylcholine receptor expressed in CHO cells. *Biochem J* **293:**495–499.
Nahorski SR, Young KW, Challiss RAJ, and Nash MS (2003) Visualizing phosphoinositide signalling in single neurons gets a green light. *Trends Neurosci* **26:**444–452.
Nash MS, Schell MJ, Atkinson PJ, Johnston NR, Nahorski SR, and Challiss RAJ (2002) Determinants of metabotropic glutamate receptor-5-mediated Ca^{2+} and inositol 1,4,5-trisphosphate oscillation frequency. Receptor density versus agonist concentration. *J Biol Chem* **277:**35947–35960.
Nash MS, Young KW, Challiss RAJ, and Nahorski SR (2001) Intracellular signalling. Receptor-specific messenger oscillations. *Nature (Lond)* **413:**381–382.
Offermanns S (2003) G-proteins as transducers in transmembrane signalling. *Prog Biophys Mol Biol* **83:**101–130.
Saxena S, Jonsson ZO, and Dutta A (2003) Small RNAs with imperfect match to endogenous mRNA repress translation. Implications for off-target activity of small inhibitory RNA in mammalian cells. *J Biol Chem* **278:**44312–44319.
Snove O and Holen T (2004) Many commonly used siRNAs risk off-target activity. *Biochem Biophys Res Commun* **319:**256–263.
Taylor CW and Thorn P (2001) Calcium signalling: IP_3 rises again. . . and again. *Curr Biol* **11:**R352–R355.
Thomas AP, Bird GS, Hajnoczky G, Robb-Gaspers LD, and Putney JW (1996) Spatial and temporal aspects of cellular calcium signaling. *FASEB J* **10:**1505–1517.
Tovey SC and Willars GB (2004) Single-cell imaging of intracellular Ca^{2+} and phospholipase C activity reveals that RGS 2, 3 and 4 differentially regulate signaling via the $G\alpha_{q/11}$-linked muscarinic M_3 receptor. *Mol Pharmacol* **66:**1453–1464.
Vickers TA, Koo S, Bennett CF, Crooke ST, Dean NM, and Baker BF (2003) Efficient reduction of target RNAs by small interfering RNA and RNase H-dependent antisense agents. A comparative analysis. *J Biol Chem* **278:**7108–7118.
Willets J and Kelly E (2001) Desensitization of endogenously expressed δ-opioid receptors: no evidence for involvement of G protein-coupled receptor kinase 2. *Eur J Pharmacol* **431:**133–141.
Young KW, Nash MS, Challiss RAJ, and Nahorski SR (2003) Role of Ca^{2+} feedback on single cell inositol 1,4,5-trisphosphate oscillations mediated by G-protein-coupled receptors. *J Biol Chem* **278:**20753–20760.
Young SH, Wu SV, and Rozengurt E (2002) Ca^{2+}-stimulated Ca^{2+} oscillations produced by the Ca^{2+}-sensing receptor require negative feedback by protein kinase C. *J Biol Chem* **277:**46871–46876.

Address correspondence to: Prof. R. A. J. Challiss, Department of Cell Physiology and Pharmacology, University of Leicester, Maurice Shock Medical Sciences Building, University Road, Leicester, LE1 9HN, UK. E-mail: jc36@le.ac.uk